PHYSOR 2012 – Advances in Reactor Physics – Linking Research, Industry, and Education
Knoxville, Tennessee, USA, April 15-20, 2012, on CD-ROM, American Nuclear Society, LaGrange Park, IL (2012)

CONSTRUCTION OF ACCURACY-PRESERVING SURROGATE FOR THE EIGENVALUE RADIATION DIFFUSION AND/OR TRANSPORT PROBLEM

Congjian Wang and Hany S. Abdel-Khalik*
Department of Nuclear Engineering
North Caroline State University
Raleigh, NC 27695
cwang21@ncsu.edu ; abdelkhalik@ncsu.edu

ABSTRACT

The construction of surrogate models for high fidelity models is now considered an important objective in support of all engineering activities which require repeated execution of the simulation, such as verification studies, validation exercises, and uncertainty quantification. The surrogate must be computationally inexpensive to allow its repeated execution, and must be computationally accurate in order for its predictions to be credible. This manuscript introduces a new surrogate construction approach that reduces the dimensionality of the state solution via a range-finding algorithm from linear algebra. It then employs a proper orthogonal decomposition-like approach to solve for the reduced state. The algorithm provides an upper bound on the error resulting from the reduction. Different from the state-of-the-art, the new approach allows the user to define the desired accuracy a priori which controls the maximum allowable reduction. We demonstrate the utility of this approach using an eigenvalue radiation diffusion model, where the accuracy is selected to match machine precision. Results indicate that significant reduction is possible for typical reactor assembly models, which are currently considered expensive given the need to employ very fine mesh many group calculations to ensure the highest possible fidelity for the downstream core calculations. Given the potential for significant reduction in the computational cost, we believe it is possible to rethink the manner in which homogenization theory is currently employed in reactor design calculations.

Key Words: ROM, RSM, POD, range-finding algorithm, active subspace

1. INTRODUCTION

The trade-off between accuracy and computational efficiency has always played an essential role in real world engineering calculations. As the accuracy requirements become more stringent, the complexity of the models continues to increase which is a reflection of the more detailed strategies employed to calculate the solution or the more detailed models representing our improved understanding about the physical phenomena. The complexity of the models often increases at a higher rate than the increase in computer power which renders their repeated execution for engineering purposes computationally inefficient or impractical. To combat this challenge, scientists have invested into two major strategies: (a) strategies to accelerate the solution of the complex model's equations via development of better solution algorithms, i.e., alternative numerical and discretization schemes; and (b) strategies to develop computationally efficient models with reduced complexity and acceptable accuracy. The later approach is referred to as 'reduced order modeling' (ROM) which represents the subject of this manuscript.

* Corresponding author: Tel.: +1 919 515 4600; fax: +1 919 515 5115

ROM methods have been developed by many computational scientists and practitioners from many different backgrounds [1]. The less complex models generated by ROM methods are often referred to as surrogate models and sometimes meta-models. Response surface methods (RSM) represent the most prominent ROM approach for building surrogates at the response level. Examples of RSM methods include polynomial chaos, stochastic collocation, regression techniques, and generalized Fourier expansions [2-5].This type of reduction has been very popular as it requires no intimate knowledge of the models being reduced. It requires only a nonintrusive access to the model where it is executed in a forward manner a number of times. Next, an assumed surface is used to find the best fit between the model predicted responses and those predicted by assumed surface. The efficiency of the RSM methods depends on the number of original model executions that must be completed to find an RSM model with acceptable accuracy. Generally, for models with many input parameters, RSM methods prove to be computationally inefficient.

Projection methods, also referred to as reduced basis methods in some communities, represent the most successful approach when reduction is done at the state level. Projection-type methods are all based on the premise that the variability of the state can be well approximated by a subspace. This means that despite the high dimensional nature of the state, it only varies along a subspace of smaller dimension, which if identified, can be used to transform the problem into one with smaller dimensions. Approximate balanced truncation methods [6], Krylov-subspace methods [7], Proper Orthogonal Decomposition (POD) [8] are examples of projection methods done at the state level. This type of reduction has been primarily exercised to accelerate the convergence of the solution, especially for models where the state must be evaluated at many points in the phase space. By performing the reduction, the computational overhead becomes dependent on the dimension of the subspace in the reduced model versus the number of state points in the original model.

In earlier work, the subspace determined by projection methods is used to reduce the dimensionality of the forward model at the reference parameters values only [6-8]. Recently, people start to construct the subspace to capture the variability of the solution for all possible parameters perturbations [9-13]. We present in this manuscript an ROM approach that constructs a surrogate in the state space with the objective to reduce the computational cost required to find the state variations for all possible parameters perturbations under which the high fidelity model is expected to be exercised.

2. STATE-BASED SURROGATE MODELING

2.1. Model Description

Consider a generalized eigenvalue problem

$$\mathbf{L}(u)\phi = \lambda \mathbf{F}(u)\phi \tag{1}$$

where one can consider $\mathbf{L} \in \mathbb{R}^{n\times n}$, and $\mathbf{F} \in \mathbb{R}^{n\times n}$ are matrix operators that describe the numerically-discretized neutron transport loss and production operators, respectively; λ is the

largest eigenvalue (equal to $1/k_{eff}$) associated with the eigenvector $\phi \in \mathbb{R}^n$ which denotes the state (i.e. the flux for neutron diffusion theory) and sometimes called the fundamental forward flux solution. The $\mathbf{L}, \mathbf{F}$ and λ are dependent on the *p* model parameters described by a vector $u \in \mathbb{R}^p$.

Now, consider a response *R* that is a linear functional of the flux:

$$R = \Sigma(u)^T \phi \tag{2}$$

with constraints:

$$\Sigma_N{}^T \phi = N \tag{3}$$

where $\Sigma(u)$ is a vector whose elements are dependent on the parameters. The Σ_N is a vector of weights that determine the normalization condition and *N* is the normalization constant.

2.2. Surrogate Model Construction

Early works show that all possible perturbed fluxes belong to a small active subspace of size *r*, and any response variation due to any parameter perturbation can be easily determined by solving *r* adjoint equations employing *r* active responses [9,10]. If *r* is much smaller than *n* (the size of the state space), one can recast the solution of Eq. (1) in terms of a set of *r* base vectors belong to the active subspace. In doing so, one recognizes that the remaining *n*-*r* directions in the state phase space cannot change the solution of Eq. (1) as the state does not vary along these directions. It is shown below that by employing only *r* base vectors, one can calculate the change in the flux due to any parameter perturbation without solving any adjoint equation.

Assume that the perturbed state/flux varies along a subspace $\mathbb{C}$ which is spanned by a basis or *r* independent vectors: $\{\theta_1, \theta_2, \cdots, \theta_r\}$. Let the set of vectors: $\{\theta_{r+1}, \theta_{r+2}, \cdots, \theta_n\}$ represents a basis for the complementary subspace $\mathbb{C}^\perp$ in $\mathbb{R}^n$ such that

$$\mathbb{C} \oplus \mathbb{C}^\perp = \mathbb{R}^n$$

Now consider a general perturbation in the input parameters, the perturbed eigenvalue problem is given by:

$$\tilde{\mathbf{L}}(\tilde{u})\tilde{\phi} = \tilde{\lambda}\tilde{\mathbf{F}}(\tilde{u})\tilde{\phi} \tag{4}$$

where '~' indicates the perturbed terms and the corresponding perturbed flux can be rewritten as:

$$\tilde{\phi} = \left(\mathbf{\Theta}\mathbf{\Theta}^T + \mathbf{\Theta}^\perp\mathbf{\Theta}^{\perp T}\right)\tilde{\phi} = \mathbf{\Theta}\mathbf{\Theta}^T\tilde{\phi} \tag{5}$$

where $\boldsymbol{\Theta} = [\theta_1, \theta_2, \cdots, \theta_r]$ and $\boldsymbol{\Theta}^{\perp} = [\theta_{r+1}, \theta_{r+2}, \cdots, \theta_n]$ are orthonormal matrices such that $\boldsymbol{\Theta}\boldsymbol{\Theta}^T + \boldsymbol{\Theta}^{\perp}\boldsymbol{\Theta}^{\perp T} = \mathbf{I}$ is the identity matrix. To find the active subspace, we employ a range-finding algorithm to identifying its effective range that may be spanned by the columns of an orthonormal matrix $\boldsymbol{\Theta} \in \mathbb{R}^{n \times r}$.

In earlier work, the size of the active subspace was identified via numerical experimentations [14]. Chaturantabut and Sorensen mentioned a heuristic estimation of the error bound which provide a reasonable qualitative estimate of the expected error. However, it is clearly not a rigorous bound [13]. In recent years, applied mathematicians were able to show that rigorous error bounds could be established using the following idea to construct the active subspace [15]. We briefly discuss how these bounds could be constructed, and refer the reader to Ref. [15] for excellent review on the mathematical literature on range-finding algorithms.

Consider a matrix $\mathbf{A}$ where one is interested in identifying its effective range spanned by the columns of an orthonormal matrix $\boldsymbol{\Theta} \in \mathbb{R}^{n \times r}$ such that some user-defined tolerance is satisfied in an upper bound sense, i.e., $\left\| \left(\mathbf{I} - \boldsymbol{\Theta}\boldsymbol{\Theta}^T \right) \mathbf{A} \right\| \le \varepsilon$. It can be shown via the algorithm below that the range could be identified using randomized matrix vector products of the form: $\mathbf{A}p_i$ where p_i is randomly generated:

(a) Form a random vector p_i, and calculate $q_i = \mathbf{A}p_i$
(b) Using a Gram-Schmidt or other orthogonalization algorithm, calculate θ_i such that: $\theta_i^T \theta_j = \delta_{ij}$ and $\text{span}\{\theta_1, ..., \theta_i\} = \text{span}\{q_1, ..., q_i\}$.
(c) Append the column θ_i to form: $\boldsymbol{\Theta}_i = [\theta_1 \quad ... \quad \theta_i] \in \mathbb{R}^{n \times i}$
(d) Calculate: $q_i^{\perp} = \left(\mathbf{I} - \boldsymbol{\Theta}_{i-1}\boldsymbol{\Theta}_{i-1}^T \right) q_i$
(e) If $\left\| q_i^{\perp} \right\| \le \varepsilon$, stop, otherwise let $i = i + 1$ and go to step (a)

This algorithm constructs a set of random vectors q_i which belong to the range of the matrix $\mathbf{A}$. The algorithm is terminated when a new vector has only a small component orthogonal to the subspace spanned by the previous vectors. The ε tolerance could be selected to match the stopping criterion for the flux that is employed in forward calculation to terminate the iterative process. After a certain rank *r* is identified by the above algorithm, an upper bound on the error could be rigorously established as follows:

(a) Pick a small integer *s*; $s = 10$ is often very conservative.
(b) Pick a sequence of *s* random Gaussian vectors $\{\upsilon_i\}_{i=1}^{s}$
(c) Calculate $z_i = (\mathbf{I} - \boldsymbol{\Theta}\boldsymbol{\Theta}^T)\mathbf{A}\upsilon_i$ for $i = 1, ..., s$, where $\boldsymbol{\Theta}$ is identified by the algorithm above and has dimensions $n \times r$
One can show that with probability at least $1 - 10^{-s}$, the following statement is true:

$$\left\|(\mathbf{I}-\boldsymbol{\Theta}\boldsymbol{\Theta}^T)\mathbf{A}\right\| \le 10\sqrt{\frac{2}{\pi}}\max_{i=1,\ldots,s}\left\|z_i\right\| \tag{6}$$

This statement allows one to define an upper bound on the error resulting from approximating the range of the matrix **A** by a subspace of size *r*. We denote the right hand side of Eq. (6) as the theoretical error:

$$\varepsilon_{\text{theory}} = 10\sqrt{\frac{2}{\pi}}\max_{i=1,\ldots,s}\left\|z_i\right\| \tag{7}$$

Note that the computational cost of implementing this range-finding algorithm is proportional to the cost of generating *r*+*s* matrix-vector products. Earlier works show that these matrix-vector products could be emulated by executing the forward model *r*+s times, each with a random input parameters perturbation [9, 10]. The power of this algorithm is that it finds a hard upper-bound on the error. This allows the analyst to decide on the maximum allowable error a priori and employ the algorithm to pick the minimum rank *r* that satisfies this error criterion.

Combining Eq. (4) and Eq. (5) gives

$$\mathbf{P}\tilde{\mathbf{L}}\left(\tilde{u}\right)\boldsymbol{\Theta}\boldsymbol{\Theta}^T\tilde{\phi} = \tilde{\lambda}\mathbf{P}\tilde{\mathbf{F}}\left(\tilde{u}\right)\boldsymbol{\Theta}\boldsymbol{\Theta}^T\tilde{\phi} \tag{8}$$

where $\mathbf{P}\in\mathbb{R}^{r\times n}$ is the preconditioner, and we choose $\mathbf{P}=\boldsymbol{\Theta}^T$ for simplicity, thus Eq. (8) becomes

$$\boldsymbol{\Theta}^T\tilde{\mathbf{L}}\left(\tilde{u}\right)\boldsymbol{\Theta}\boldsymbol{\Theta}^T\tilde{\phi} = \tilde{\lambda}\boldsymbol{\Theta}^T\tilde{\mathbf{F}}\left(\tilde{u}\right)\boldsymbol{\Theta}\boldsymbol{\Theta}^T\tilde{\phi} \tag{9}$$

Let $\hat{\mathbf{L}}=\boldsymbol{\Theta}^T\tilde{\mathbf{L}}\boldsymbol{\Theta}, \hat{\mathbf{F}}=\boldsymbol{\Theta}^T\tilde{\mathbf{F}}\boldsymbol{\Theta},$ and $\hat{\phi}=\boldsymbol{\Theta}^T\tilde{\phi}$, therefore, the surrogate model can be written as

$$\hat{\mathbf{L}}\hat{\phi} = \hat{\lambda}\hat{\mathbf{F}}\hat{\phi} \tag{10}$$

where $\hat{\mathbf{L}}\in\mathbb{R}^{r\times r}, \hat{\mathbf{F}}\in\mathbb{R}^{r\times r}, \hat{\phi}\in\mathbb{R}^{r}$ and $\hat{\lambda}$ is the eigenvalue for the surrogate model.

2.3. State-Based Surrogate Modeling Algorithm

The algorithm for state-base surrogate modeling can be summarized as follows:

step 1: Random perturb the input parameter within certain ranges.

step 2: Employing range-finding algorithm to construct the active subspace $\{\theta_i\}_{i=1}^{r}$ such that:

$\boldsymbol{\Theta}=\left[\theta_1,\theta_2,\cdots,\theta_r\right]\in\mathbb{R}^{n\times r}, \boldsymbol{\Theta}^T\boldsymbol{\Theta}=\mathbf{I}_{r\times r},$ and $R(\boldsymbol{\Theta})=R\{\theta_1,\cdots,\theta_r\}$;

step 3: Construct the surrogate operator $\hat{\mathbf{L}}=\boldsymbol{\Theta}^T\tilde{\mathbf{L}}\boldsymbol{\Theta},$ and $\hat{\mathbf{F}}=\boldsymbol{\Theta}^T\tilde{\mathbf{F}}\boldsymbol{\Theta}$;

step 4: Solve the surrogate model $\hat{\mathbf{L}}\hat{\phi}=\hat{\lambda}\hat{\mathbf{F}}\hat{\phi}$ for $\hat{\lambda}$ and $\hat{\phi}$;

step 5: Calculate the unnormalized perturbed flux $\tilde{\phi}_u = \boldsymbol{\Theta}\hat{\phi}$;

step 6: Renormalize the perturbed flux $\tilde{\phi} = \frac{N}{S_N{}^T \tilde{\phi}_u}\tilde{\phi}_u$.

Note that the bulk of the computational burden in this algorithm is in step 1 where the forward model is executed *r* times. The surrogate model can be easily solved if the size of the active subspace *r* is a small number. The rest of the computational burden involves only linear algebra operations which are computationally cheap when compared to the cost of executing the forward and/or adjoint model for uncertainty quantification.

3. NUMERICAL EXPERIMENTS

Two case studies are analyzed using MATLAB code. The first case is a seven-group diffusion model in 1-D slab geometry with two fuel assemblies [16], and the length of each mesh is 0.09 cm. The state is described by the seven-group flux solution, and

$$\phi = \left[\phi_1{}^1 \cdots \phi_{224}{}^1 \cdots \phi_1{}^g \cdots \phi_{224}{}^g \cdots \phi_1{}^7 \cdots \phi_{224}{}^7 \right] \in \mathbb{R}^{1568\times 1}$$

where the superscript denotes the energy group, and the subscript denotes the mesh number. We denote the fast group as the first four energy groups, and the thermal group as the left three energy groups. The responses represent the perturbed flux values at each point in the phase space, and we also define the thermal total flux value as: $\phi_{th} = \sum_{g=4}^{7}\sum_{i=1}^{224}\phi_i{}^g$. The input parameters are represented by the seven-group cross sections. The model schematic is shown in Fig. 1. The cross sections are given in [17].

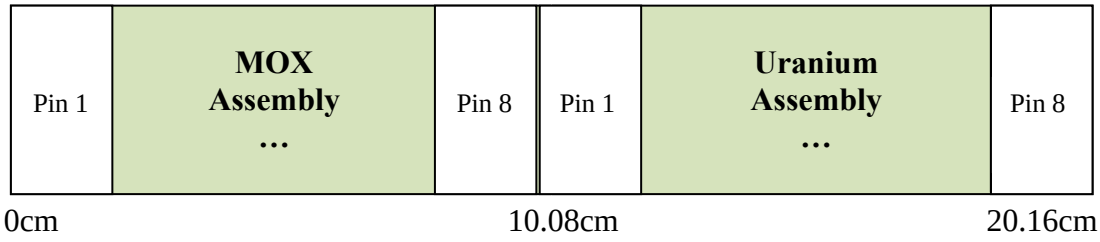

Fig. 1a 7 Core Model

Pin 1 MOX 8.7%	**Pin 2** MOX 8.7%	**Pin 3** Guide Tube	**Pin 4** MOX 8.7%	**Pin 5** MOX 8.7%	**Pin 6** Guide Tube	**Pin 7** MOX 7.0%	**Pin 8** MOX 4.3%

Fig. 1b Design of the MOX Assembly

Pin 1	Pin 2	Pin 3	Pin 4	Pin 5	Pin 6	Pin 7	Pin 8
UO_2	UO_2	Guide Tube	UO_2	UO_2	Guide Tube	UO_2	UO_2

Fig. 1c Design of the Uranium Assembly

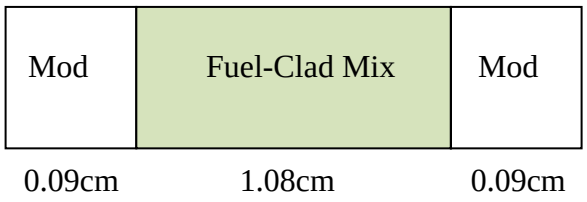

Fig. 1d Pin Cell Design

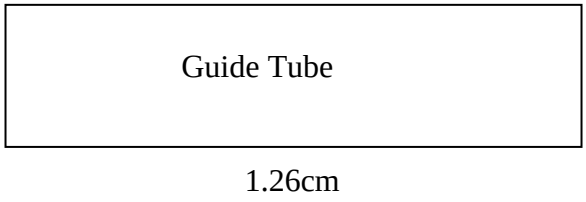

Fig. 1f Guide Tube

Figure 1. Seven Group Diffusion Model Layouts

The responses represent the perturbed flux values in the phase space. The state-based surrogate modeling algorithm is executed, and is tested for a perturbed model such that all cross sections perturbations were randomly selected from uniform distribution within 10% relative to their reference values. The exact perturbed responses are calculated using direct forward perturbation which requires a full forward model execution. Fig. 2 compares the real errors in the flux (*rms*) calculated by the surrogate model to the theoretical error predicted by randomized range-finding algorithm. The *x*-axis in Fig. 2 runs from 1 to 1568 over all space-energy indices for the flux, and errors in this figure are defined as

$$rms = \sqrt{\frac{1}{N \times G} \sum_{g=1}^{G} \sum_{i=1}^{N} \left(\frac{\phi_{i,\,\text{exact}}{}^{g} - \phi_{i,\,\text{approx}}{}^{g}}{\Phi_{average}} \right)^2}$$

where N=224 denotes the total mesh points, G=7 denotes the total energy groups, $\Phi_{average}$ denotes the average unperturbed flux value over all phase space points, and $\varepsilon_{\text{theory}}$ is given in Eq. 7. In order to compare the real error to the theoretical error, we normalize the theoretical error in the following way

$$rms_{\text{theory}} = \frac{\varepsilon_{\text{theory}}}{\Phi_{average} \sqrt{N \times G}}$$

To check the adequacy of surrogate model for severe flux variations, the methodology is also employed to estimate perturbed flux resulting from the insertion of a control rod. The control rod is simulated by significantly increasing the absorption cross-section in pin cell 3 in MOX assembly. Fig. 3 shows the result in a similar manner to Fig. 2. Despite the huge change in the eigenvalue (approximately a 63% change from the reference value 1.0650), the state-based surrogate algorithm is able to calculate the perturbed flux below user-defined tolerance.

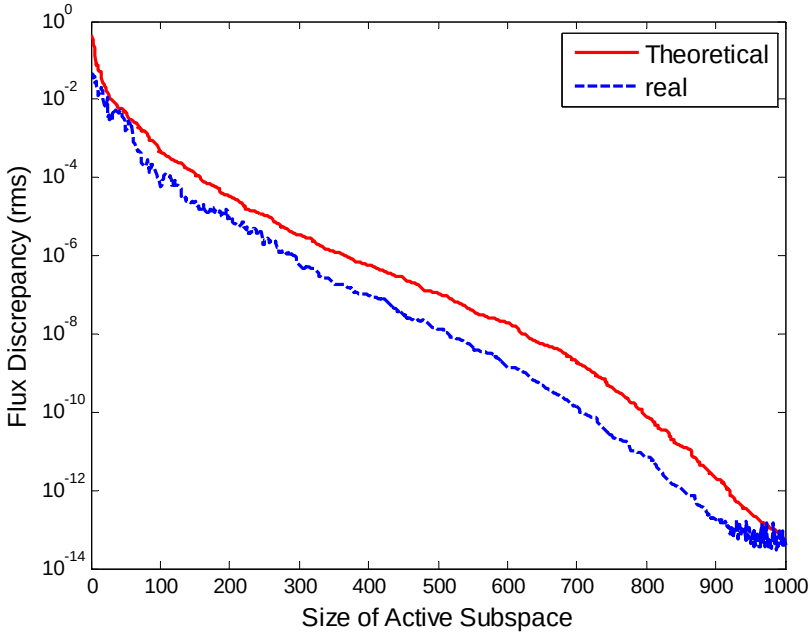

Figure 2. Comparisons of Flux Discrepancy versus *r* for 7 group

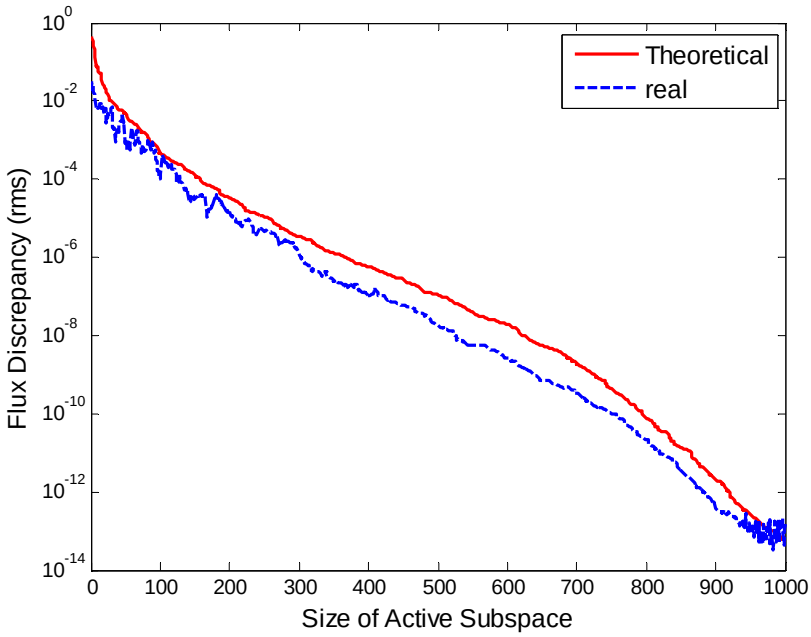

Figure 3. Comparisons of Flux Discrepancy versus *r* for 7 group (w/ CR insertion)

The second case is a two-group diffusion model with cross-sections condensed from the previous seven-group employing the flux distribution calculated from the previous diffusion model. Similar to previous case, the responses represent the perturbed flux values in the phase space. The state-based surrogate modeling algorithm is executed, and is tested for a perturbed model such that all cross sections perturbations were randomly selected from uniform distribution

within 10% relative to their reference values. The exact perturbed responses are calculated using direct forward perturbation which requires a full forward model execution. To understand the impact of energy condensation on the size of the active subspace, we employ the same model schematic as shown in Fig. 1. Fig. 4 shows the result in a similar manner to Fig. 2. For the sake of comparision, Let us pick user-defined error tolerance, say $rms = 10^{-6}$. From Figs. 2 and 4 the corresponding sizes of the active subspace to meet this error tolerance is 93 and 365, respectively. Moreover, Fig. 5 shows the size of active subspace is almost linear dependent on the number of energy groups with lower order accuracy. This results implies that we can also employ the low-fidelity model to predict the size of active subspace for the high-fidelity model without execute the high-fidelity complex model over and over again. An interesting observation is that the size of the active subspace for the high fidelity is approximately 3.5 times higher than the low fidelity model. Recall that the high fidelity model is based on 7 groups whereas the low fidelity is based on 2 groups. This demonstrates that the reduction preserves the additional degrees of freedom employed by the high fidelity model to improve the accuracy of the model. Note that the 7G model employs additional degrees of freedom in the form of the scattering block where neutrons are allowed to scatter up and down between the various groups. Therefore, the degrees of freedom can be reduced if the scattering cross-sections are not perturbed. Fig. 6 shows the reductions on the degrees of freedom compared to Fig. 5. If however the high fidelity model does not introduce any new information that are relevant to the responses of interest, the size of the reduced model will not increase. This was illustrated in a previous paper with the high fidelity model employing a fine mesh [9].

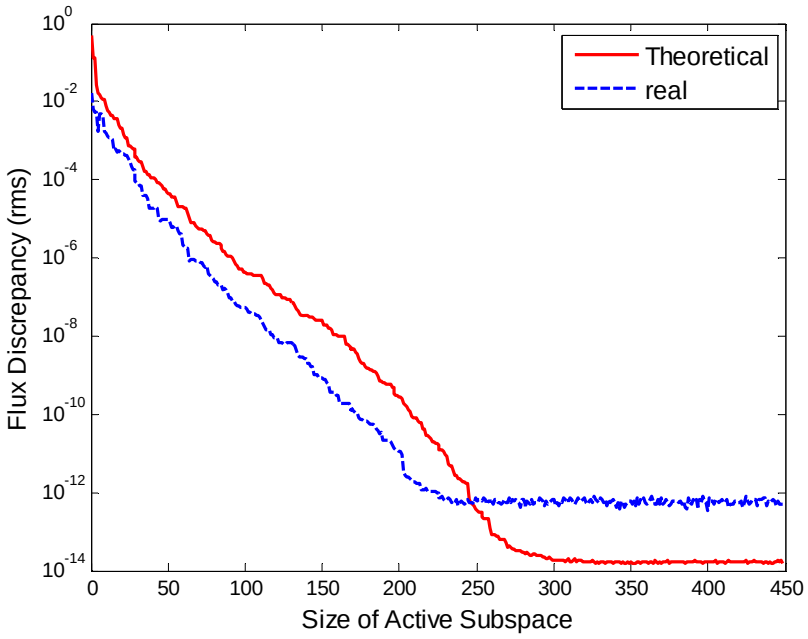

Figure 4. Comparisons of Flux Discrepancy versus *r* for 2 group

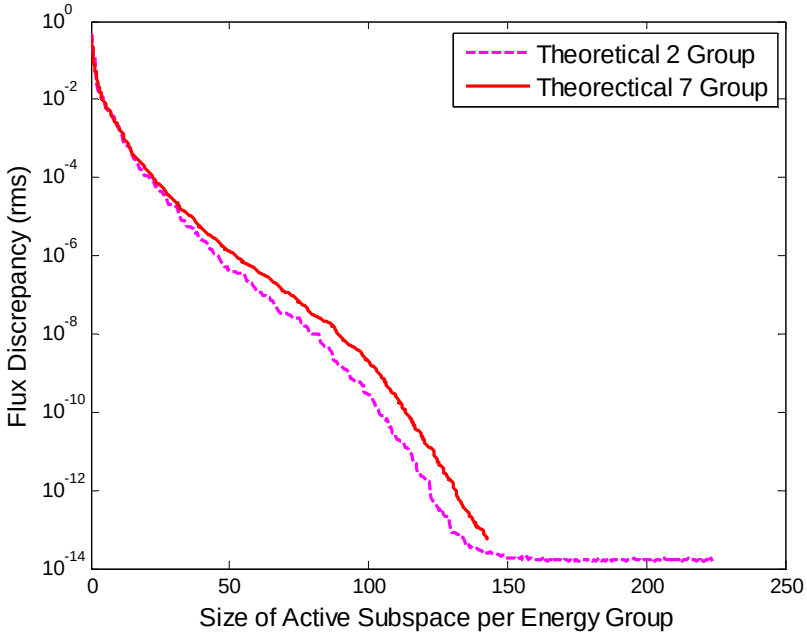

Figure 5. Analysis of Size of Active Subspace versus Energy Group

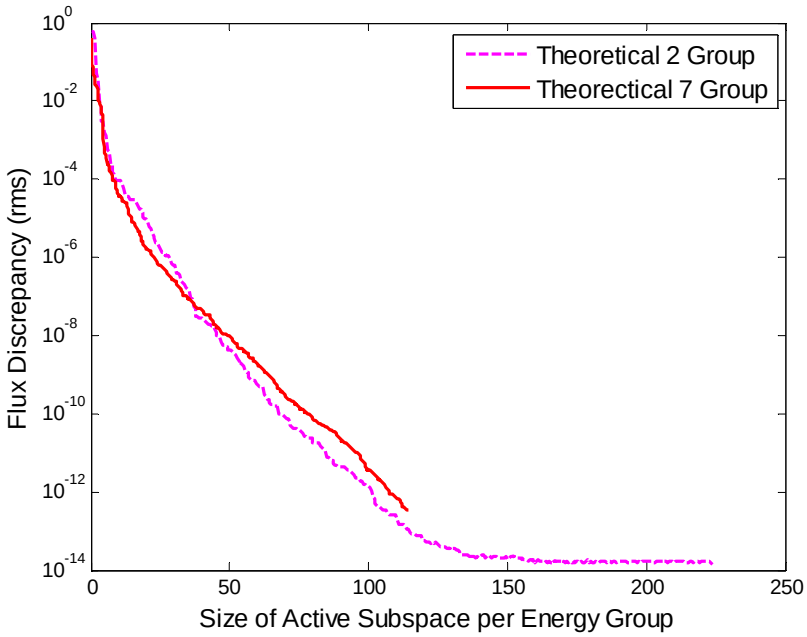

Figure 6. Analysis of Size of Active Subspace versus Energy Group (without Perturbing Scattering Cross-Sections)

Next, Fig. 7 compares the relative discrepancies in the eigenvalues between two-group diffusion model and seven-group diffusion model, and Fig. 8 compares the relative discrepancies in the thermal total flux value between the two models.

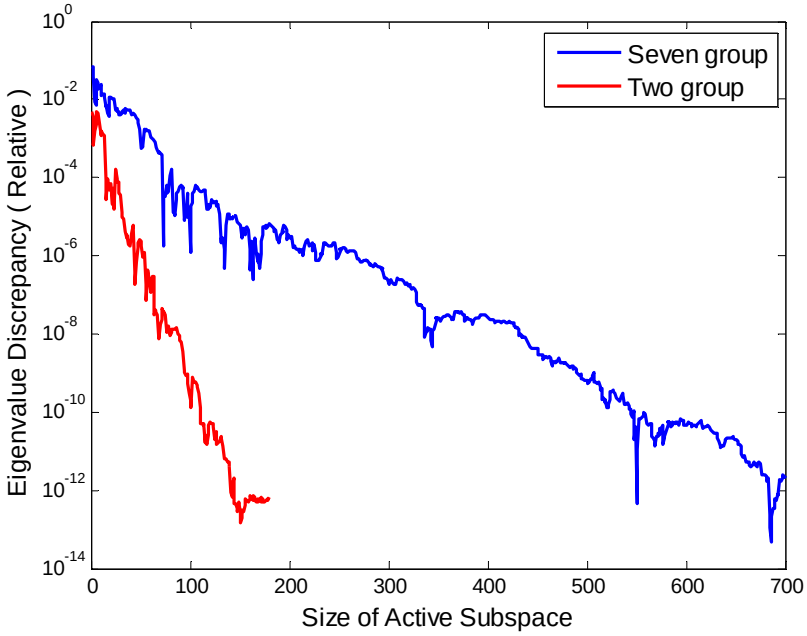

Figure 7. Analysis of Surrogate Model Errors versus *r* (Eigenvalue)

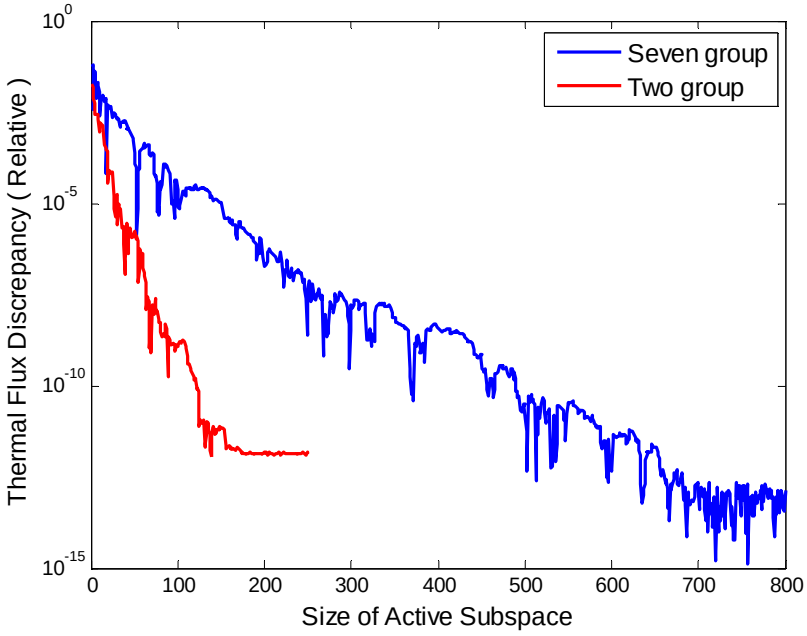

Figure 8. Analysis of Surrogate Model Errors versus *r* (Thermal Total Flux)

4. CONCLUSIONS

A new approach has been developed for the order reduction for *K*-eigenvalue problem with many input parameters and output responses. This new approach may be viewed as a hybrid between the POD method of snapshots and the range-finding algorithms. The idea is to build a surrogate model by employing the active subspace to identify all important variations in the perturbed state

inherent in the original complex model. This is achieved by projecting the original operator onto the active subspace, and solving the surrogate eigenvalue problem only in this active subspace. By restricting the solution to only an active subspace, the new method may be viewed as an effective way to boost the performance of uncertainty quantification on the original complex model. Moreover, rigorous upper bound on the error can determined for the surrogate model.

ACKNOWLEDGMENTS

This work was supported by the Consortium for Advanced Simulation of Light Water Reactors, an Energy Innovation Hub for Modeling and Simulation of Nuclear Reactors under U. S. Department of Energy Contract No. DE-AC05-00OR22725.

REFERENCES

1. A. C. Antoulas, D. C. Sorensen, and S. Gugercin , "A survey of model reduction methods for large scale systems", *Journal of Contemporary Mathematics*, **280**, (2001).
2. B. M. Adams, W. J. Bohnhoff, et al., DAKOTA: A multilevel parallel object-oriented framework for design optimization, parameter estimation, uncertainty quantification, and sensitivity analysis: Version 5.0 users manual, Tech. Rep. SAND2010-2183, Sandia National Laboratories, December (2009).
3. M. J. Lighthill, *Introduction to Fourier Analysis and Generalised Functions*, Cambridge, England: Cambridge University Press, (1958).
4. R.G. Ghanem, P.D. Spanos, *Stochastic Finite Elements: A Spectral Approach*, Courier Dover Publications, (1991).
5. D. Xiu, *Numerical Methods for Stochastic Computations: A Spectral Method Approach*, Princeton University Press, (2010).
6. T. Penzl, "Algorithms for Model Reduction of Large Dynamical Systems", *Linear Algebra and its Applications*, **415** (2006).
7. K. Gallivan, E. Grimme, and P. Van Dooren, "Pade Approximation of Large-Scale Dynamic Systems with Lanczos Methods", *Proceedings of the 33rd IEEE Conference on Decision and Control*, (1994).
8. P. Holmes, J. Lumley, and G. Berkooz, *Turbulence, Coherent Structures, Dynamical Systems and Symmetry*, Cambridge Monographs on Mechanics, Cambridge University Press, (1996).
9. C. J., Wang, H. S. Abdel-Khalik, "Exact-to-Precision Generalized Perturbation Theory for Source-Driven Problem," *Nucl. Eng. Des.* (2011), doi: http://dx.doi.org/10.1016/j.nucengdes.2011.09.009
10. C. J. Wang, and H. S. Abdel-Khalik, "Exact-to-Precision Generalized Perturbation Theory for Eigenvalue Problem," *Nucl. Eng. Des.* 2011 (Submitted)
11. C. J. Wang and H. S. Abdel-Khalik, "Order Reduction Approach for Generalized Perturbation Theory," *2011 ANS Winter Meeting and Nuclear Technology Expo*, Washington DC, Omni Shoreham Hotel, October 30 – November 3, 2011
12. Y. S. Bang and H. S. Abdel-Khalik, "State-Based Adjoint Model Reduction for Large Scale Control Problems," *4th International Symposium on Resilient Control Systems, ISRCS 2011*, Boise, Idaho, August 9-11, 2011
13. S. Chaturantabut, and D. C. Sorensen, "Nonlinear Model Reduction Via Discrete Empirical Interpolation," *SIAM J. Sci. Comput*. **Vol. 32**, No. 5, pp 2737-2764 (2010).

14. H.S. Abdel-Khalik, “Adaptive Core Simulation”, PhD Dissertation, North Carolina State University, (2004).
15. N. Halko, P. G. Martinsson, and J. A. Tropp, “Finding Structure with Randomness: Probabilistic Algorithms for Constructing Approximate Matrix Decompositions,” *SIAM Rev.*, Survey and Review Section, June 2011.
16. D. Y. Anistratov, “Multilevel Quasidiffusion Methods for Solving Multigroup Neutron Transport *k*-Eigenvalue Problems in One-Dimensional Slab Geometry,” *Nucl. Sci. Eng.*, **169** (2011).
17. E. E. Lewis, M. A. Smith, N. Tsoulfanidis, G. Palmiotti, T. A. Taiwo & R. N. Blomquist. “Benchmark specification for Deterministic 2-D/3-D MOX fuel assembly transport calculations without spatial homogenization (C5G7),” Expert Group on 3-D Radiation Transport Benchmarks, NEA/NSC/DOC(2001)4. (c5g7)